

Supporting Information

*Hao Sun, Yishu Jiang, Longbin Qiu, Xiao You, Jiahua Yang, Xuemei Fu, Peining
Chen, Guozhen Guan, Zhibin Yang, Xuemei Sun, Huisheng Peng**

*State Key Laboratory of Molecular Engineering of Polymers, Collaborative
Innovation Center of Polymers and Polymer Composite Materials, Department of
Macromolecular Science and Laboratory of Advanced Materials, Fudan University,
Shanghai 200438, China; E-mail: penghs@fudan.edu.cn.*

*Author to whom correspondence should be addressed.

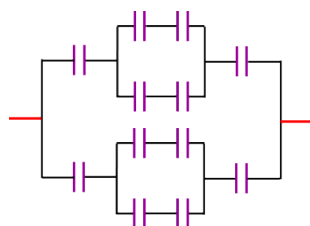
E-mail Address: penghs@fudan.edu.cn

Preparation of the self-healing polymer (SHP) substrate.

The SHP was synthesized via a modified Leibler's method.^{S1-S3} 22.8 g of DM-80 (85 wt% diacids and 10 wt% triacids, donated by Demand Chemical Co., Ltd, Shanghai) was reacted with 9 g of diethylenetriamine at 160 °C under stirring at an argon atmosphere. The resulting product was dissolved in 100 mL of chloroform and washed with 100 mL of deionized water and 50 mL of methanol, followed by removal of the residual chloroform by a rotary evaporation. The purified product (1 g) was further dissolved in chloroform (10 mL) to form a uniform solution. This solution was dip-coated onto clean glass slides, followed by evaporation of the solvent at 25 °C for 2 h and heated to 80 °C for 30 min to completely remove the solvent and form a uniform film.

Calculation of the discharge time ratio of the supercapacitors in Figures 3b and 3i.

Assuming that all supercapacitor units share a capacitance of C_0 , the capacitance of the supercapacitor in Figure 3b (C_{3b}) is $1/2C_0$. The equivalent circuit diagram of the supercapacitor in Figure 3i can be simplified below.



The capacitance (C_{3i}) is calculated to be $2/3C_0$, and the ratio of the capacitance (C_{3i}/C_{3b}) is 1.33. The discharge time ($t_{discharge}$) can be calculated from the equation of $C = I \times t_{discharge} / V$, where I and V are the discharge current and voltage variation during galvanostatic discharge process, respectively. Because of the same discharge current and voltage applied for the supercapacitors in Figures 3b and 3i, the ratio of the discharge time is calculated to be 1.33, which equals to the ratio of the capacitance (C_{3i}/C_{3b}).

Calculation of the energy density and power density of the fusible supercapacitors based on CNT/PANI composite film.

The energy density (E , Wh kg^{-1}) is calculated from the following equation:^{S4}

$$E = \frac{1}{8} C_{electrode} V^2 \times \frac{1000}{3600}$$

where $C_{electrode}$ is the specific capacitance of electrode ($F g^{-1}$), V is the potential

window (V).

The power density (P, W kg⁻¹) is calculated from the following equation using galvanostatic charge-discharge curves with different discharge current densities:^{S5}

$$P = \frac{E}{t} \times 3600$$

where E (Wh kg⁻¹) is the energy density, and t is the discharging time.

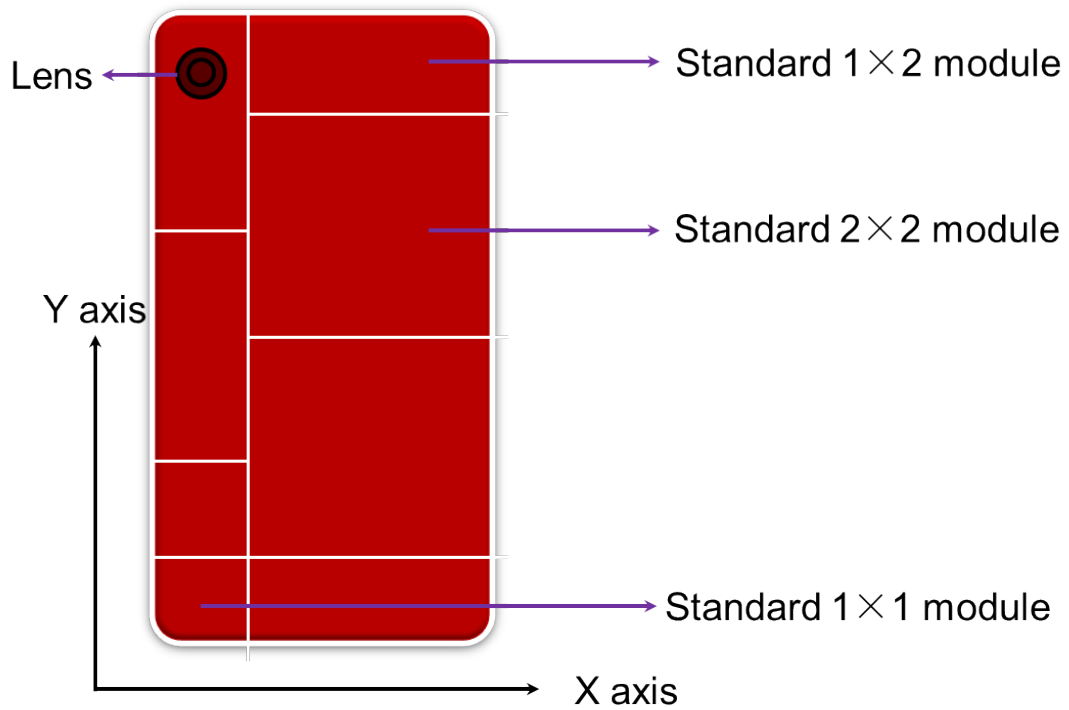


Figure S1. Schematic illustration to a modular smartphone with standardized modules that allow easy assembly, high customisation and simple upgrade according to the Google modular smartphone.

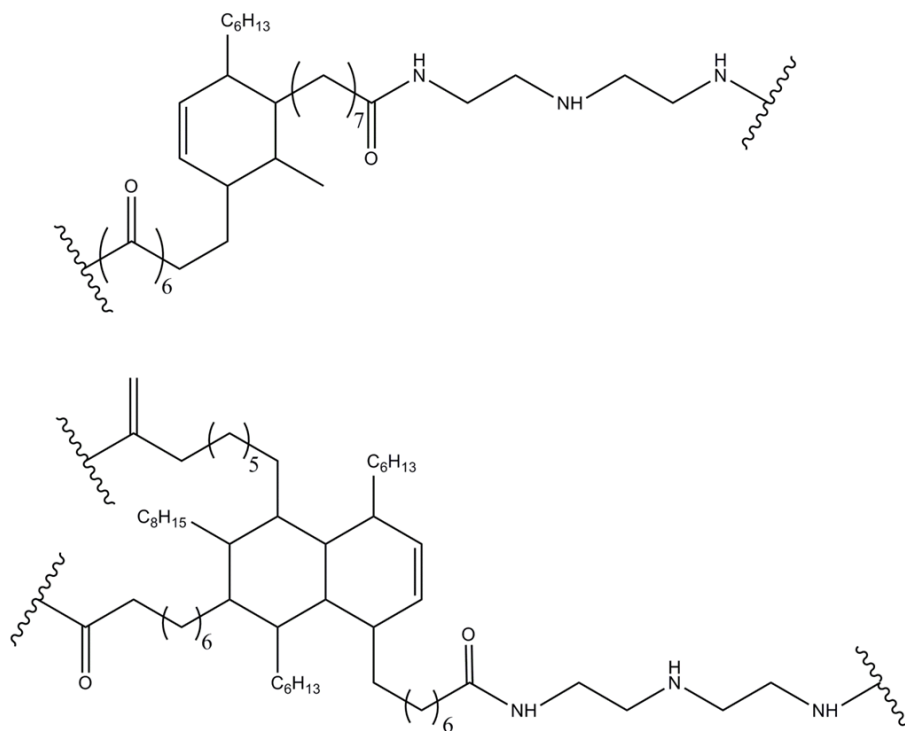


Figure S2. Chemical structure of the SHP.

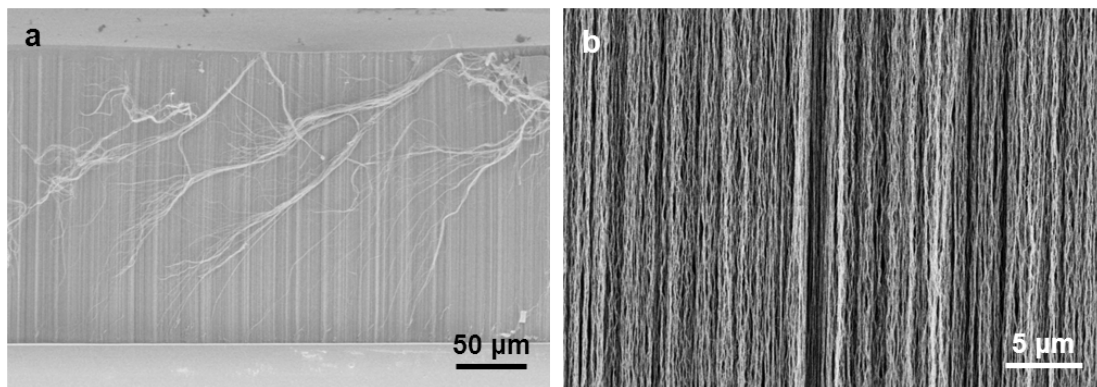


Figure S3. SEM images of a spinnable CNT array at low and high magnifications.

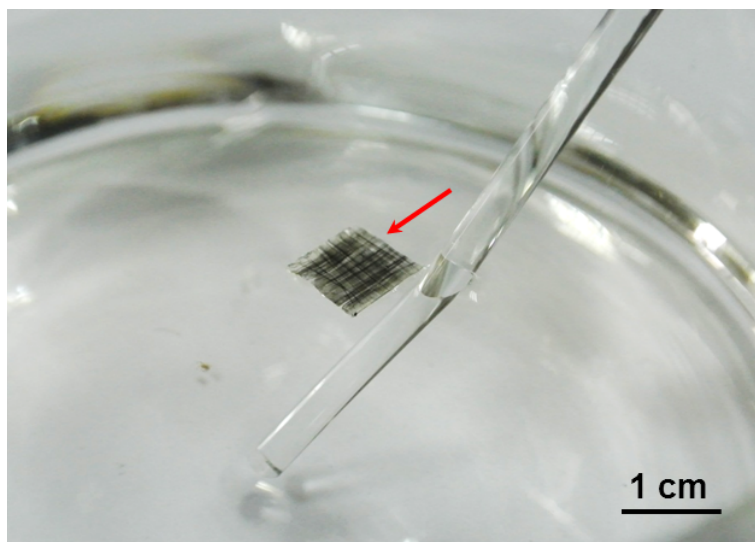


Figure S4. Photograph of an aligned CNT/SHP film floated on water. The arrow showed the CNT/SHP film.

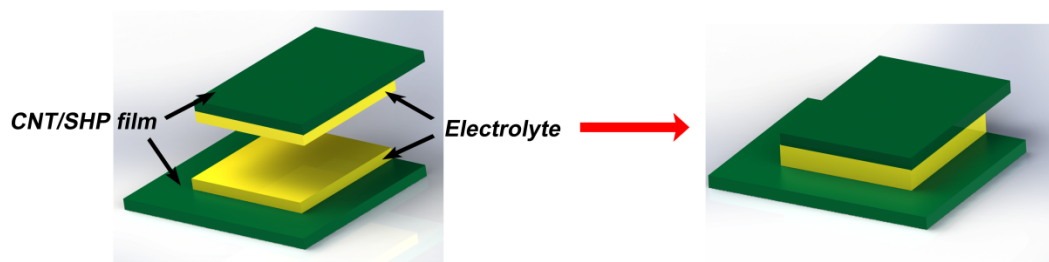


Figure S5. Schematic illustration to the fabrication of a typical fusible supercapacitor.

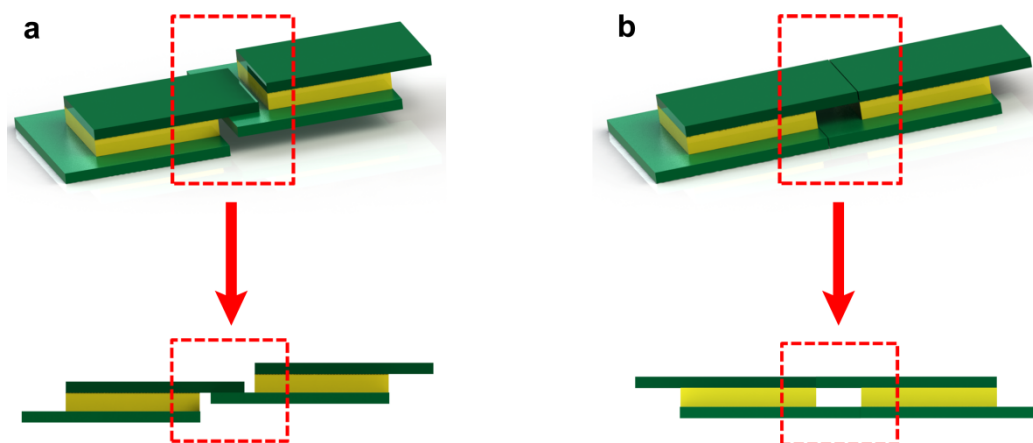


Figure S6. Schematic illustration to the connection in series (**a**) and in parallel (**b**) of fusible supercapacitors. The labelled rectangles by dashed red lines at **a** and **b** correspond to the connected areas of fusible supercapacitors in series and in parallel, respectively.

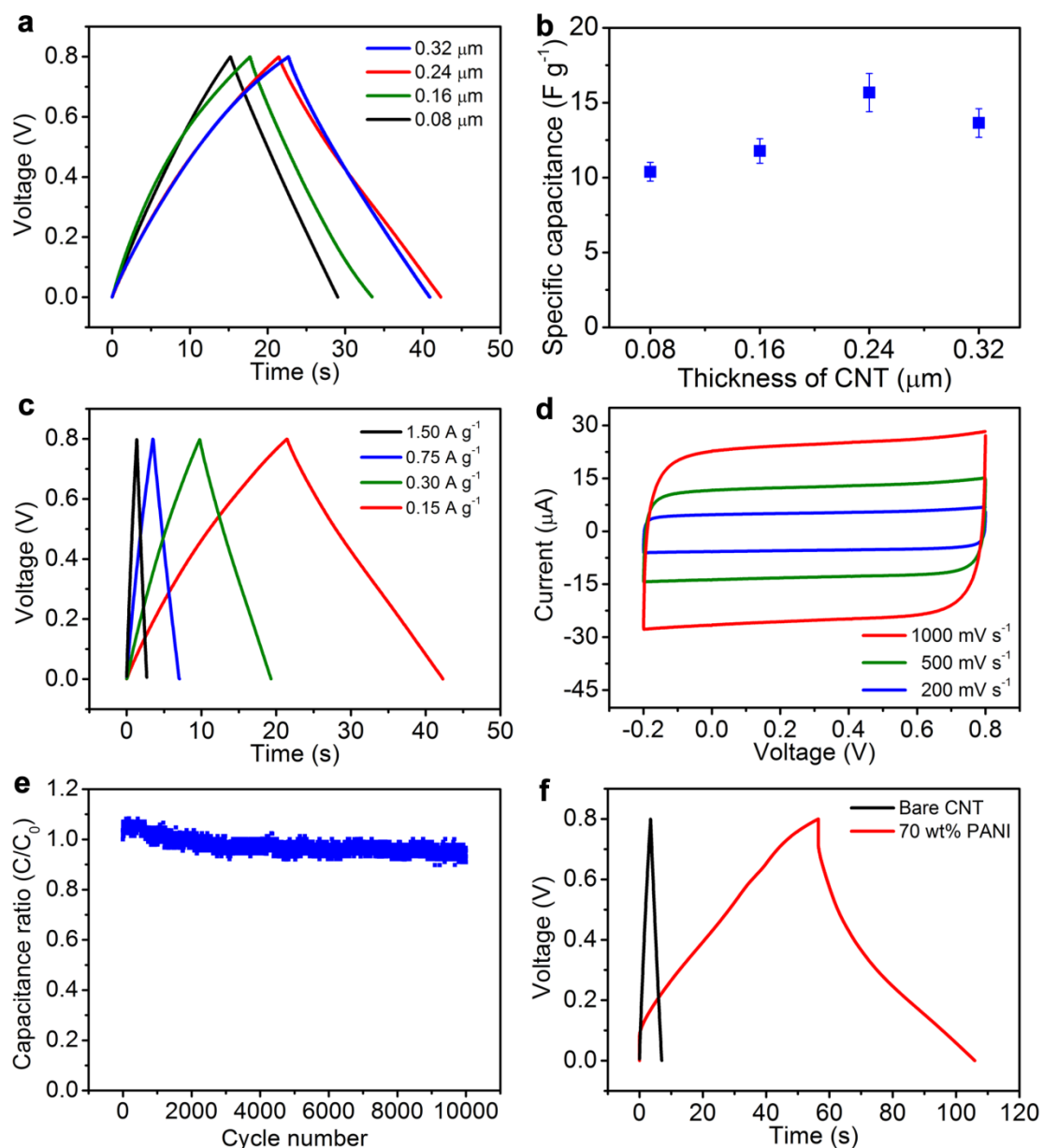


Figure S7. Capacitive performances of the fusible supercapacitors. **a.** Galvanostatic charge-discharge curves based on CNT sheets with increasing thicknesses from 80 to 320 nm (Current density, 0.15 A g^{-1}). **b.** Dependence of the specific capacitance on the thickness of CNT sheet. **c.** Galvanostatic charge-discharge curves with increasing current densities from 0.15 to 1.50 A g^{-1} . **d.** CV curves at increasing scan rates of 200, 500 and 1000 mV s^{-1} . **e.** Specific capacitances during 10000 charge-discharge cycles at a current density of 1.50 A g^{-1} . **f.** Galvanostatic charge-discharge curves based on bare CNT sheet and CNT/PANI (PANI weight percentage of 70%) composite film as electrodes at 0.75 A g^{-1} .

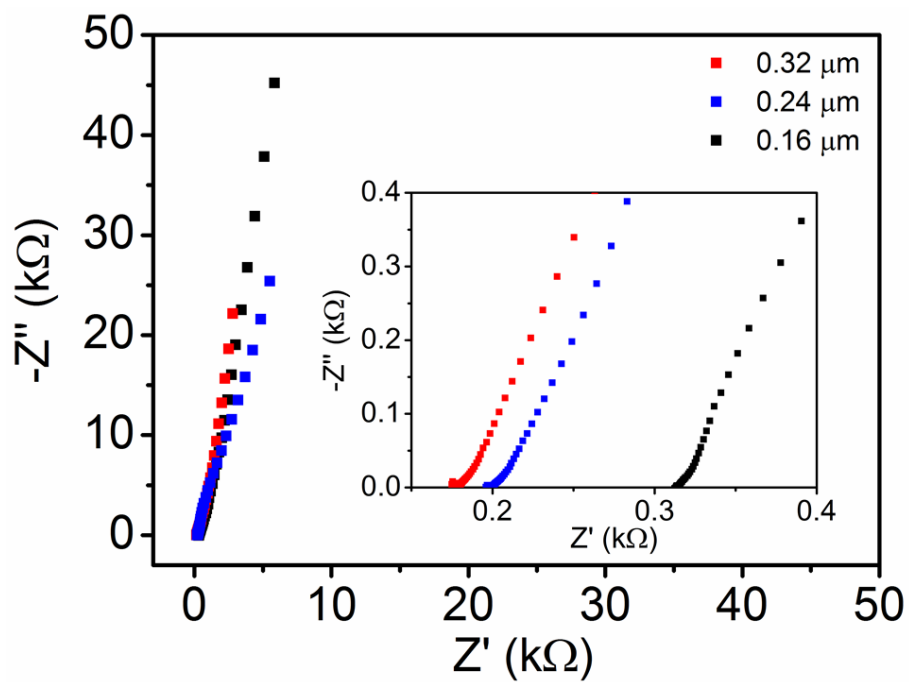


Figure S8. Nyquist plots of fusible supercapacitors consisted of electrodes with different thicknesses of CNT sheets.

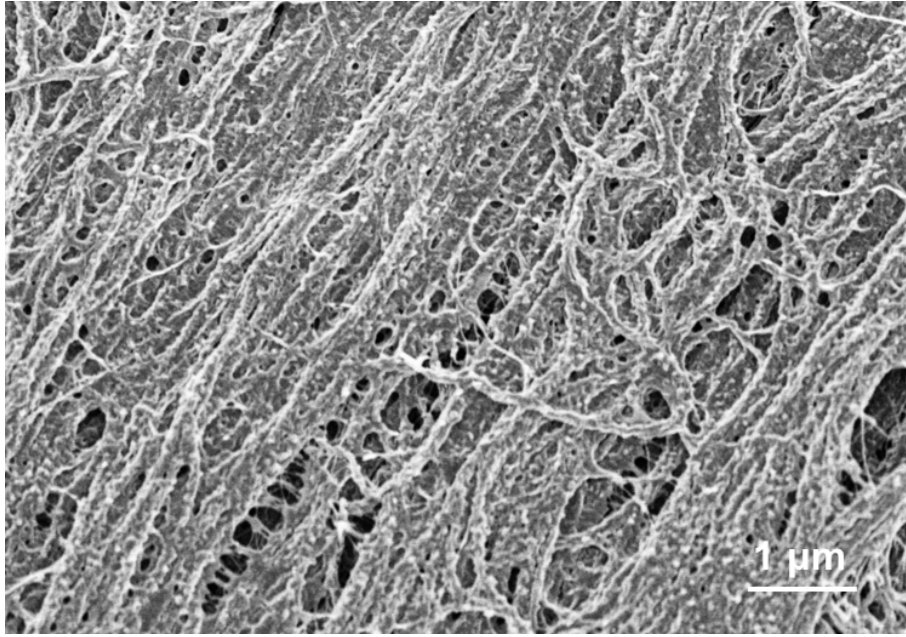


Figure S9. SEM image of a CNT/PANI composite film with PANI weight percentage of 70%.

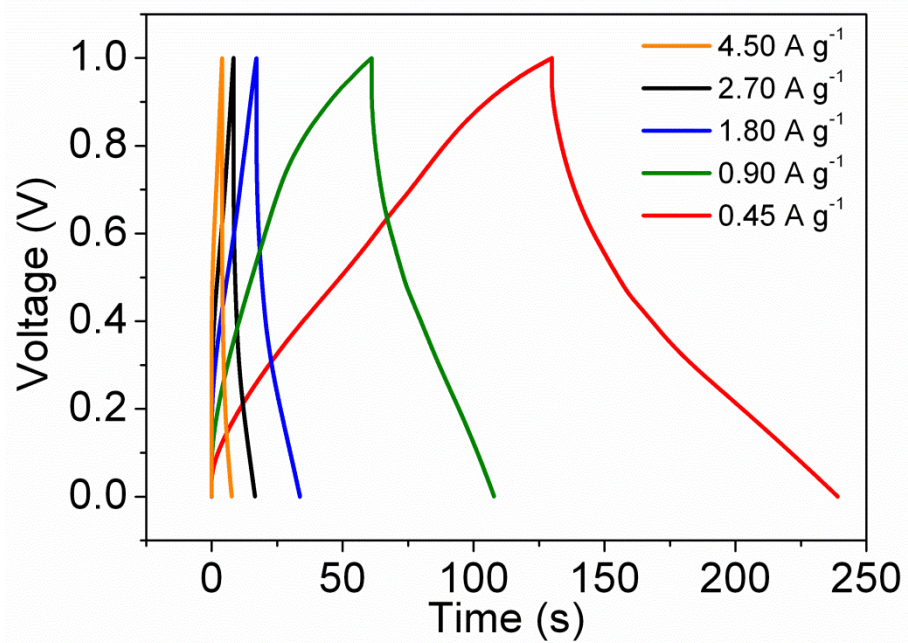


Figure S10. Galvanostatic charge-discharge curves of the fusible supercapacitors based on CNT/PANI composite films (PANI weight percentage of 70%) with increasing current densities from 0.45 to 4.50 A g⁻¹.

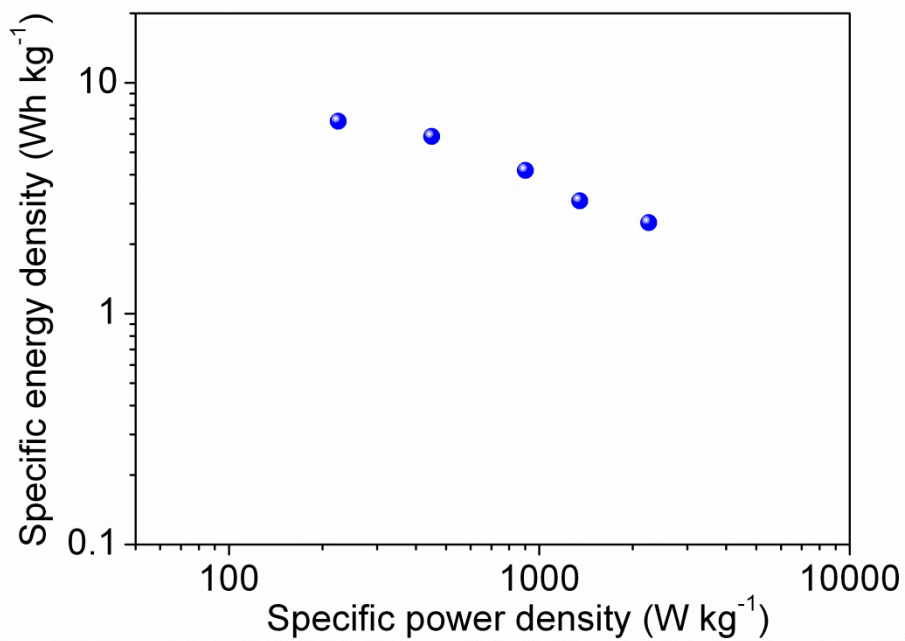


Figure S11. Ragone plot of the fusible supercapacitors based on CNT/PANI composite films (PANI weight percentage of 70%).

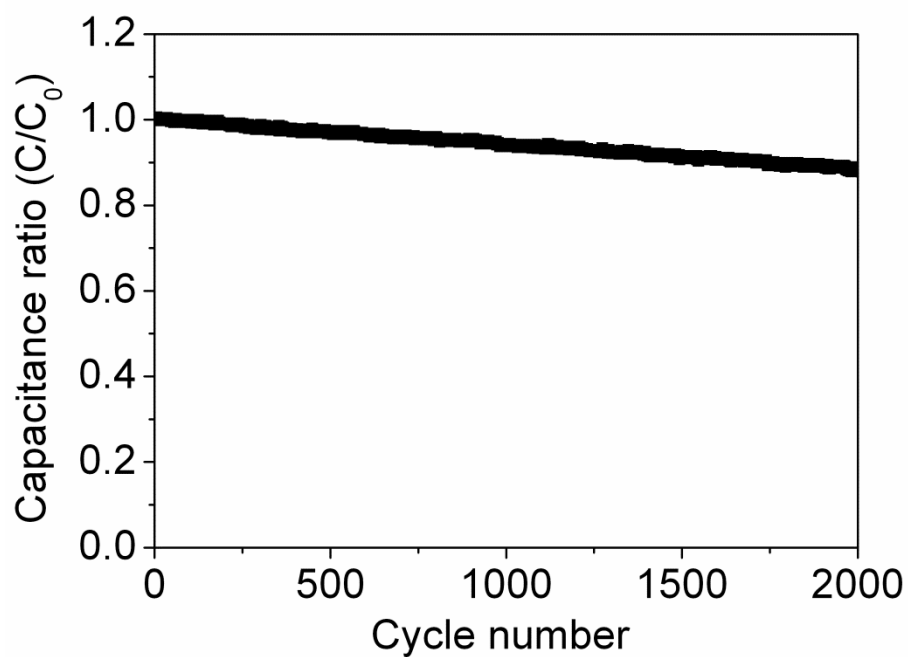


Figure S12. Specific capacitances of fusible supercapacitors based on CNT/PANI composite films (PANI weight percentage of 70%) during 2000 charge-discharge cycles at a current density of 1.80 A g^{-1}

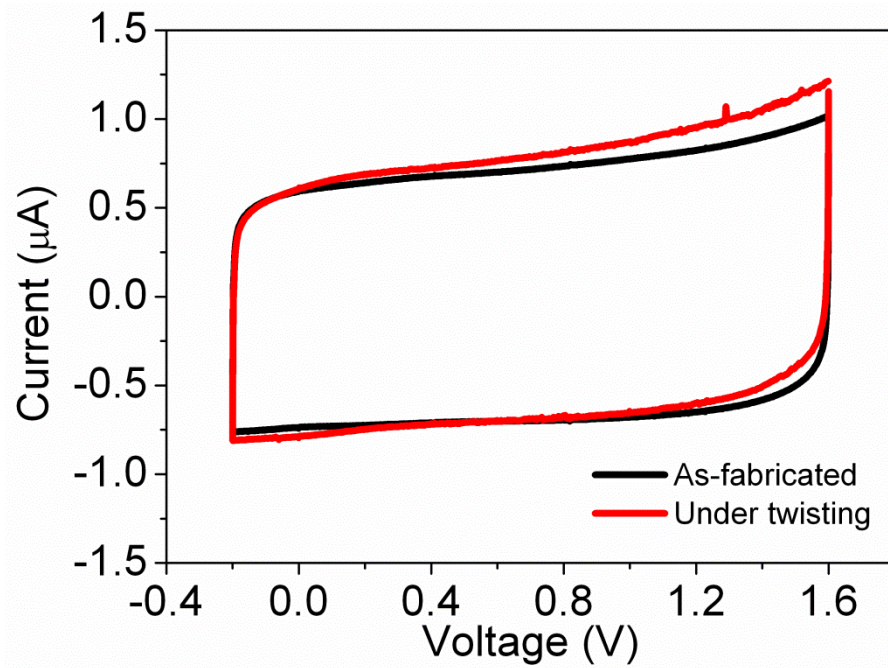


Figure S13. CV curves of two supercapacitors being connected in series before and under twisting (scan rate of 50 mV s^{-1}).

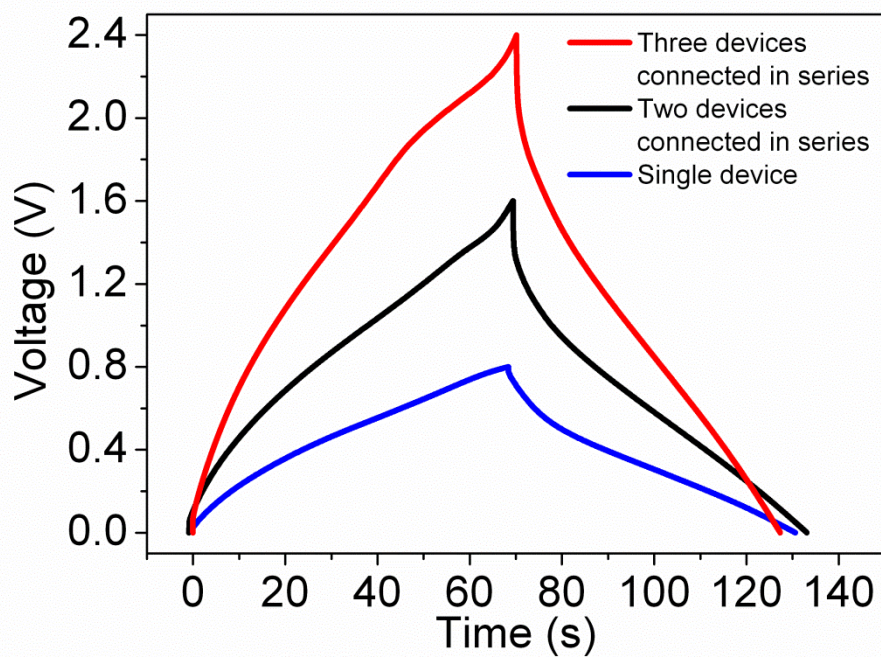


Figure S14. Galvanostatic charge-discharge curves of supercapacitors based on CNT/PANI composite films (PANI weight percentage of 70%) without and with fused connection in series. Current density, 0.6 A g^{-1} .

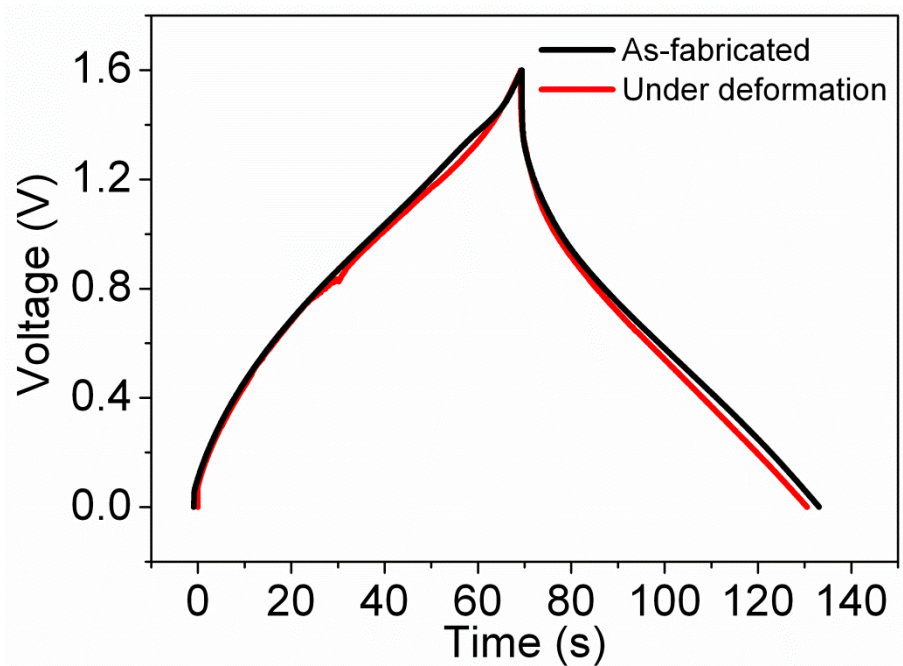


Figure S15. Galvanostatic charge-discharge of two fused supercapacitors based on CNT/PANI composite films (PANI weight percentage of 70%) without and under bending. Current density, 0.6 A g^{-1} .

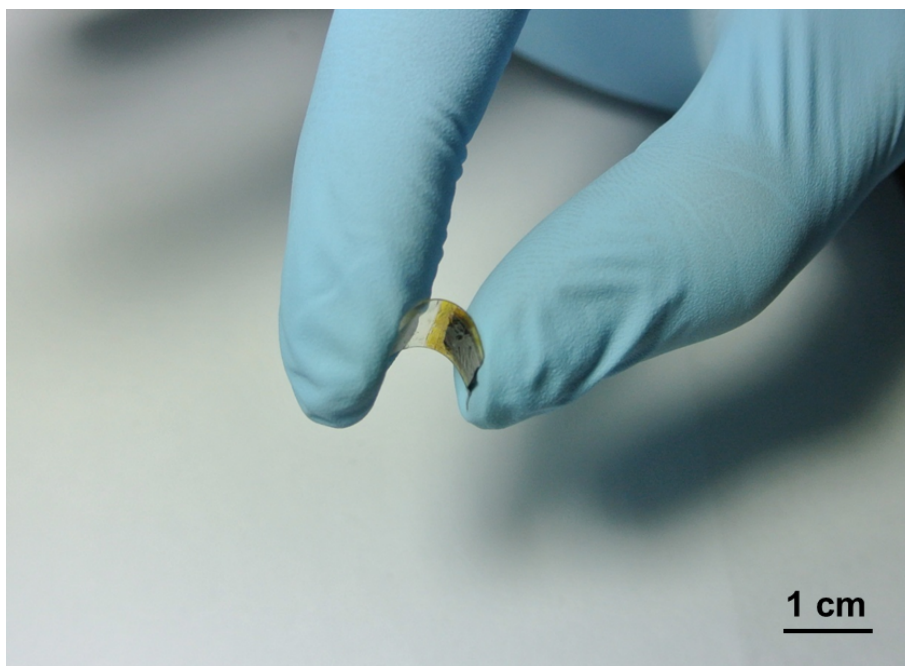


Figure S16. Photograph of a fusible perovskite solar cell under bending.

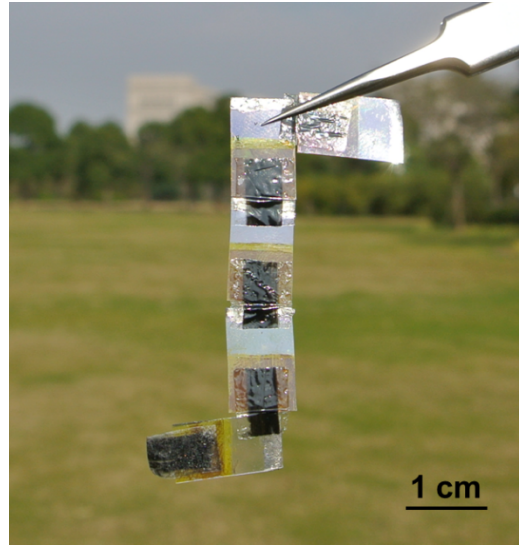


Figure S17. Photograph of five fusible perovskite solar cells being fused in series.

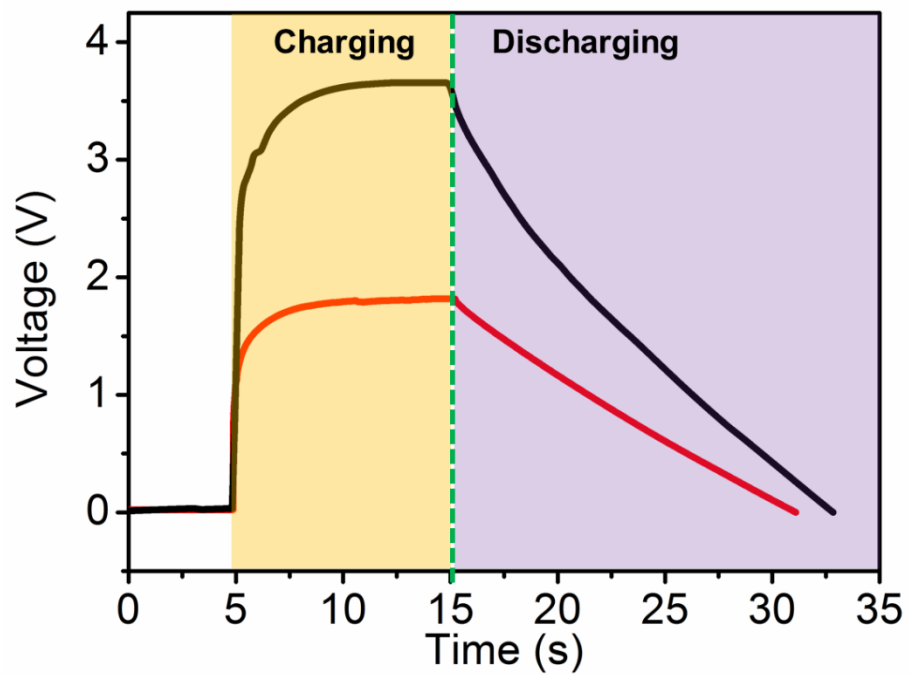


Figure S18. Photocharging and galvanostatic discharging curves of the integrated four units (red curve) and eight units (black curve) at a current density of 0.30 A g^{-1} .

References for the Supporting Information

- S1 H. Sun, X. You, Y. Jiang, G. Guan, X. Fang, J. Deng, P. Chen, Y. Luo, H. Peng, *Angew. Chem. Int. Ed.* **2014**, *126*, 9680-9685.
- S2 P. Cordier, F. Tournilhac, C. Soulié-Ziakovic, L. Leibler, *Nature* **2008**, *451*, 977-980.
- S3 B. C. Tee, C. Wang, R. Allen, Z. Bao, *Nat. Nanotechnol.* **2012**, *7*, 825-832.
- S4 J. Liu, L. Zhang, H. Wu, J. Lin, Z. Shen, X. Lou, *Energy Environ. Sci.* **2014**, *7*, 3709-3719.
- S5 D. Yu, K. Goh, H. Wang, L. Wei, W. Jiang, Q. Zhang, L. Dai, Y. Chen, *Nat. Nanotech.* **2014**, *9*, 555-562.